

Effect of gold ion concentration on size and properties of gold nanoparticles in TritonX-100 based inverse microemulsions

Tokeneer Ahmad · Irshad A. Wani · Jahangeer Ahmed · Omar A. Al-Hartomy

Received: 19 January 2013 / Accepted: 9 April 2013 / Published online: 21 April 2013
© The Author(s) 2013. This article is published with open access at Springerlink.com

Abstract Gold nanoparticles have been prepared successfully using TritonX-100 inverse microemulsion at different concentrations of HAuCl₄ (0.1, 0.05, 0.04, 0.03, 0.02 and 0.01 M). We have studied the effect of gold ion concentration on the particle size, morphology, surface area and optical properties of the gold nanoparticles. The gold nanoparticles were characterized by X-ray diffraction, transmission electron microscopy, UV–Visible spectroscopy and Brunauer–Emmett–Teller surface area analysis. X-ray diffraction studies show the monophasic nature of the gold nanoparticles. TritonX-100 stabilized gold nanoparticles were appeared to be agglomerated at higher concentrations (0.1 and 0.05 M) of Au³⁺ with an average grain size of 60 and 50 nm, respectively. Monodisperse and uniform gold nanoparticles with well-defined morphologies of an average grain size of 15 and 25 nm were obtained at lower concentrations (0.01 and 0.02 M). UV–Visible spectroscopy shows the characteristic surface plasmon resonance peak ~540 nm along with the peaks at shorter and longer wavelengths may be due to the higher order plasmon resonance of the gold nanoparticles. The surface areas of the gold nanoparticles were found to be in the

range of 5.8–107 m²/g which were well in agreement with the electron microscopic studies.

Keywords Microemulsion · Gold nanoparticles · X-ray diffraction · Transmission electron microscopy · BET surface area

Introduction

The basic research in nanoscience deals with the synthesis of nanoparticles of controlled size and morphology. Nanomaterials have attracted considerable attention in recent years because of their fundamental properties, organization to form superstructures and applications (Sastry et al. 2003). The properties of the nanomaterials originated primarily because of quantum confinement of free electrons, large surface to volume ratio and highly disordered arrangement of dipoles at the surface as compared to their bulk counterparts (Colvin et al. 1994; Alivisatos 1996). The nanoparticles find applications in optoelectronics (Colvin et al. 1994; Gracias et al. 2000), solar cells (Kamat et al. 1998), catalysis (Valden et al. 1998), nonlinear optical (Yoffe 1993) and photoelectrochemical devices (Mansur et al. 1995). Among metal nanoparticles, gold nanostructures have been extensively investigated because of their size and shape dependant surface plasmon related optical properties (Burda et al. 2005). Gold nanostructures exhibit applications in chemical inertness, biological compatibility, optical switches and molecular labeling where phenomena such as Surface Enhance Raman Scattering (SERS) can be exploited (Niemeyer 2001). Gold nanoparticles have also been used as contrast agents for optical coherence tomography (Chen et al. 2005), radiosensitizers (Chithrani et al. 2010), in

T. Ahmad (✉) · I. A. Wani
Nanochemistry Laboratory, Department of Chemistry,
Jamia Millia Islamia, New Delhi 110025, India
e-mail: tahmad3@jmi.ac.in

J. Ahmed
Department of Chemistry, Michigan State University,
East Lansing, MI 48824, USA

O. A. Al-Hartomy
Department of Physics, Faculty of Science, University of Tabuk,
Tabuk 71491, Saudi Arabia

chemotherapy (Huang et al. 2006) and therapeutic agents for photothermal cancer treatment (Takahashi et al. 2005).

Various methods based on soft chemistry route have been reported in the literature for the preparation of nanoparticles, such as sol–gel (Epifani et al. 2000), sonochemical (Wani et al. 2011; Wani and Ahmad 2013), solvothermal (Ahmad et al. 2013; Wani et al. 2010), coprecipitation (Gul et al. 2008), polymeric citrate precursor route (Al-Hartomy et al. 2012) and reverse micelles or inverse microemulsion (Wani et al. 2013) methods. During the last two decades, considerable effort has been devoted for the synthesis of gold nanoparticles, focusing on control over their size, shape, solubility, stability and functionality (Wani and Ahmad 2013). Numerous preparative methods for gold nanoparticles have also been reported (Wani and Ahmad 2013; Ahmad et al. 2013; Daniel and Astruc 2004; Turkevich et al. 1951). The size of gold nanoparticles has been controlled by varying the feed ratio of gold salt to sodium citrate (Frens 1973). Various stabilizing reagents, such as thiol ligands (Brust et al. 1994), polyethylene glycol (Haba et al. 2007), polyvinyl alcohol (Tripathy et al. 2007), polyvinyl pyrrolidone (Wagner and Kohler 2005), chitosane (Huang and Yang 2004) and surfactants (Kuo et al. 2004; Deng et al. 2005) were used to tune the size and shape of the gold nanostructures. Few reports are also available showing the formation of metal nanoparticles using TritonX-100 as the surfactant in the microemulsion system (Wani et al. 2013; Zhang and Chan 2002; Spirin et al. 2005; Zhang and Chan 2003; Lee et al. 2002).

The major challenge in the synthesis process is to control the particle size, shape and particle size distribution of the nanoparticles. Reverse micelles or microemulsions have been established as an effective and versatile method for the synthesis of various ultrafine inorganic particles with uniform shape and controlled sized distribution (Ahmad et al. 2004, 2005, 2006; Ahmad and Ganguli 2004). In this paper, we report the synthesis of gold nanoparticles using TritonX-100 inverse microemulsions at the variable concentrations of the gold salt precursor. The gold nanoparticles were characterized by X-ray diffraction studies (XRD), transmission electron microscopy (TEM), UV–Visible and Brunauer–Emmett–Teller (BET) surface area studies.

Experimental

Materials and methods

All the reagents and chemicals were of analytical grade and used without any further purification. The solutions were prepared in double distilled water. To prepare gold nanoparticles at different concentrations using TritonX-100 as

the surfactant, the six sets of microemulsions of TritonX-100/1-hexanol/cyclohexane/aqueous phase (Au^{3+}) have been prepared which were marked as A, B, C, D, E and F. In each set, the aqueous phase of first microemulsion (ME-I) contains gold metal salt, HAuCl_4 (Spectrochem, India) while the second microemulsion (ME-II) contained aqueous phase of NaBH_4 as the reducing agent. The first series of microemulsions (ME-I) differ in the molar concentration of the gold metals salt (HAuCl_4) whose concentration varies as 0.1, 0.05, 0.04, 0.03, 0.02 and 0.01 M denoted as A, B, C, D, E and F microemulsions, respectively. The second series of microemulsions (ME-II) contains sodium borohydride (NaBH_4) of the same molar concentration. These microemulsions were made up of the following compositions: 30 ml of TritonX-100 (Thomas Baker) as a surfactant, 20 ml of 1-hexanol (Spectrochem, 99 %) as a co-surfactant, 200 ml of cyclohexane (Rankem, 99 %) as an organic solvent and 10 ml of an aqueous phase. The two microemulsions in each set were mixed and then stirred for 24 h during which color changes were observed and the final color of each microemulsion is shown in Fig. 1. The size of the TritonX-100 based reverse micelles or droplets varies in the range 5–18 nm depending on the concentration of aqueous phase as observed in the region corresponding to stable reverse micelles (Kaushik et al. 2007). After mixing, the two reactants premicellized in two separate microemulsions are brought in contact with each other through inter-micellar exchange reaction. The micelles undergo numerous collisions and thereby the reactants are exchanged, mixed, and react to form the desired nanoparticles inside the reverse micelles. The size of the resultant nanoparticles increases slightly due to collision between the micelles and formation of encounter pair and subsequent conversion in fused dimer. The surface tension of the fused dimer becomes very high due to large surface area and is unable to sustain its geometry. Thus, the

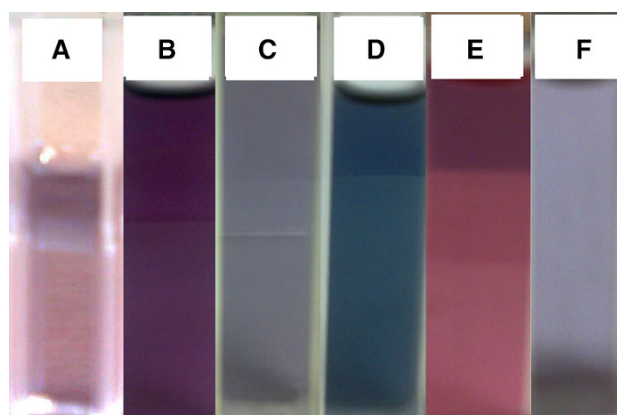


Fig. 1 Colors of the gold nanoparticles appeared in TritonX-100 based inverse microemulsions at **a** 0.1 M, **b** 0.05 M, **c** 0.04 M, **d** 0.03 M, **e** 0.02 M and **f** 0.01 M concentrations of gold salt (HAuCl_4)

fused dimer finally breaks down into two stable smaller droplets containing the precipitated material (Ganguli and Ahmad 2007). The solutions at the final stage were then centrifuged and the precipitate was washed with acetone several times to remove the surfactants and water soluble impurities. The precipitate was finally dried in an oven at 50 °C. The experimental yield was also determined and found to be ~80 % to the theoretical yield which was found to be low as compared to the solvothermally synthesized silver nanoparticles (~98 %) (Wani et al. 2010).

Instrumentation

The X-ray diffraction studies have been carried out on Bruker D8 advance X-ray diffractometer using Ni-filtered Cu-K α X-rays of wavelength (λ) = 1.54056 Å. The data were obtained at the scanning rate of 0.05°/s. The raw data obtained were subjected to the back ground correction and K α_2 reflections were stripped off using the normal stripping procedure. The micrographs were recorded on Technai G² transmission electron microscope operated at an accelerating voltage of 200 kV. The microscopic specimens were prepared by adding a drop of the dispersed sample on a porous carbon film supported on a carbon grid and dried in oven. UV–Visible spectral studies were carried out at room temperature on an ocean-optics lambda 25 spectrophotometer in the wavelength range of 200–900 nm using a quartz cuvette. The surface area analysis of the samples at the liquid nitrogen temperature (78 K) was recorded on the BET surface area analyzer procured from Quantachrome Instruments Limited (Model Nova 2000e, Make Quantachrome, USA).

Results and discussion

X-Ray diffraction (XRD) studies

The phase purity of the gold nanoparticles was confirmed by X-ray diffraction studies. Figure 2 shows the XRD overlay plots of gold nanoparticles prepared in inverse microemulsions using TritonX-100 as the surfactant at the different molar concentrations of aqueous HAuCl₄ solution. All the diffraction patterns correspond to the monophasic nanocrystalline gold. The reflections belong to [111], [200] and [220] planes could be satisfactorily indexed to the pure crystalline metallic gold with face centred cubic (fcc) structure.

Transmission electron microscopic (TEM) studies

Figures 3 and 4 show the TEM images of gold nanoparticles prepared at different molar concentrations of aqueous

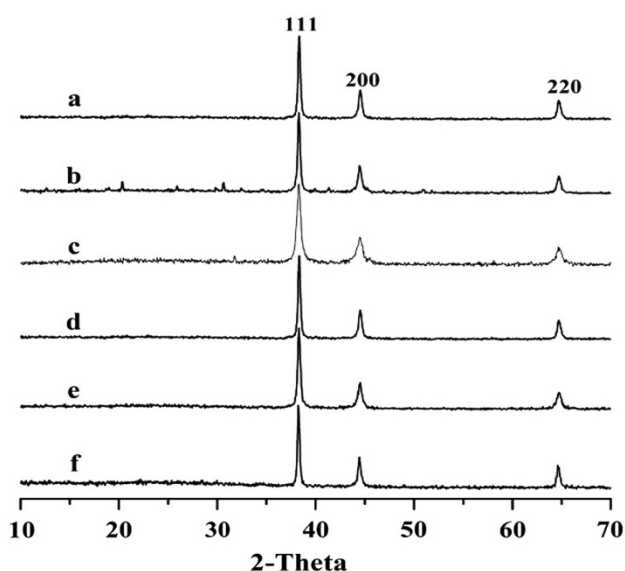
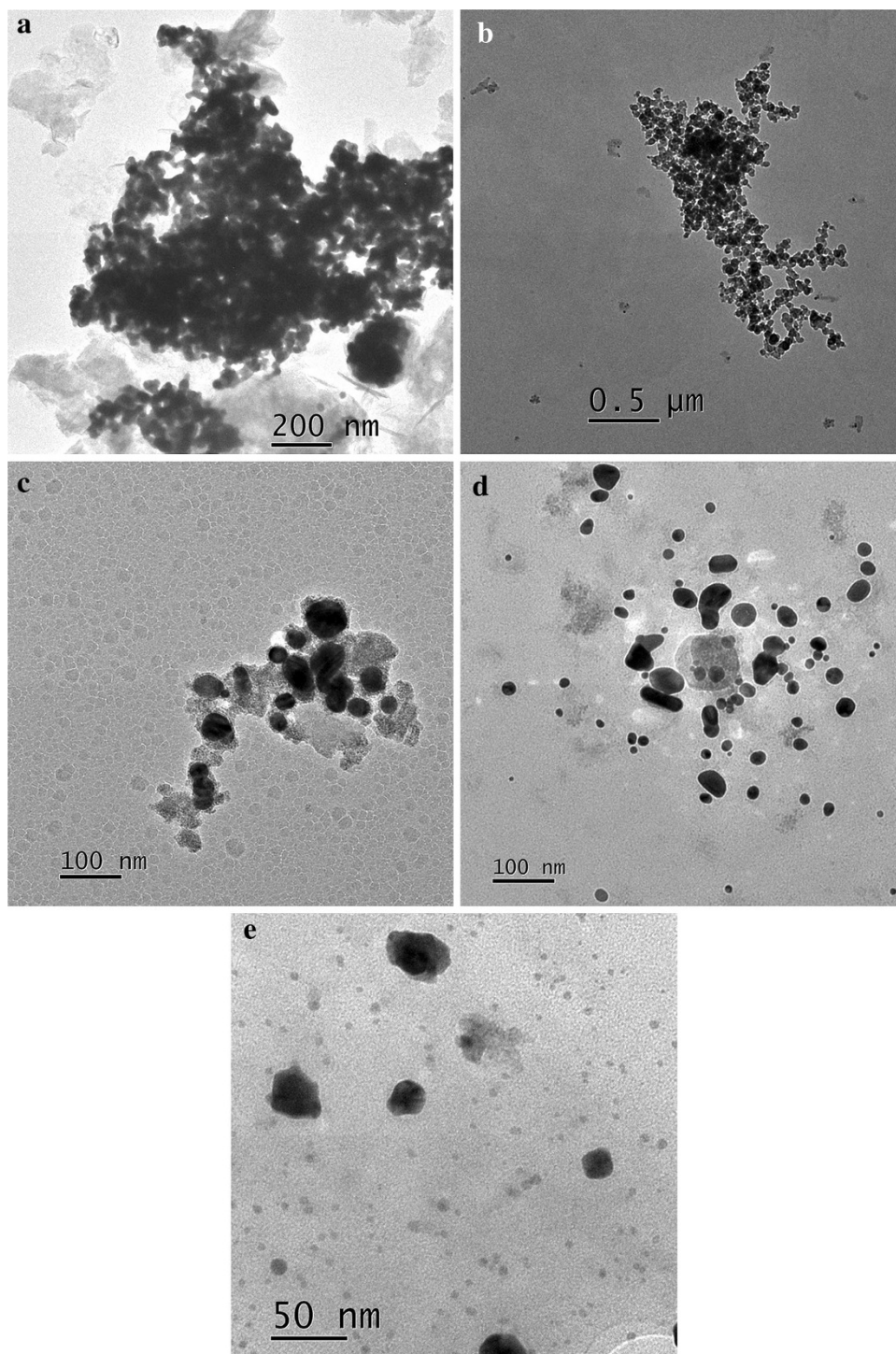


Fig. 2 X-ray diffraction patterns of gold nanoparticles prepared at **a** 0.1 M, **b** 0.05 M, **c** 0.04 M, **d** 0.03 M, **e** 0.02 M and **f** 0.01 M concentrations of HAuCl₄

HAuCl₄ solution. The gold nanoparticles prepared at 0.1 and 0.05 M concentrations of aqueous HAuCl₄ were highly agglomerated (Fig. 3a, b) with the average particle size of 60 and 50 nm, respectively. However, gold nanoparticles at 0.04 M (Au³⁺) were slightly agglomerated with an average particle size of 40 nm (Fig. 3c). Gold nanoparticles of the average size of 35 and 25 nm were obtained at the concentrations of 0.03 and 0.02 M HAuCl₄ solution inside the microemulsions as shown in Fig. 3d, e, respectively. Figure 4a, b shows the low and high magnification TEM micrographs of gold nanoparticles prepared at 0.01 M Au³⁺. As can be observed from the TEM images, the particles are highly uniform and monodisperse with nearly hexagonal morphology. The particles size histogram shows that the size of the gold nanoparticles varies in the range of 5–38 nm with an average grain size of 15 nm (Fig. 4c). The average size of the nanoparticles is well corroborated with the high magnification TEM image as shown in Fig. 4b. Note that the size of the gold nanoparticles decreases with decrease in concentration of the gold salt. Further, the extent of agglomeration was also found to be concentration dependent and the agglomeration decreases on decreasing the concentration of gold salt. The extent of agglomeration at high concentration may be associated with the high surface energy and high collision frequency of gold nanoparticles (Antunez-Garcia et al. 2011; Arcidiacono et al. 2004). As the concentration of gold salt decreases in inverse microemulsions, the number of colloid gold nanoparticles decreases in a constant volume and hence, there is a decrease in agglomeration which may lead to the formation of monodisperse and uniform gold nanoparticles at low concentrations.

Fig. 3 TEM images of the gold nanoparticles prepared at **a** 0.1 M, **b** 0.05 M, **c** 0.04 M, **d** 0.03 M and **e** 0.02 M concentrations of Au^{3+}



UV–Visible spectroscopic studies

Figure 5a–f shows the time evolution of the UV–Visible absorption spectra of the gold nanoparticles prepared in TritonX-100 based inverse microemulsions using sodium borohydride as the reducing agent at different

concentrations of gold salt. Along with the main surface plasmon absorption band located at ~ 540 nm, a second absorption band at longer wavelength ~ 670 nm in Fig. 5a–c is also observed with the progress of the reaction. The second band, which is also called the longitudinal dipole plasmon band, might be appeared due to the

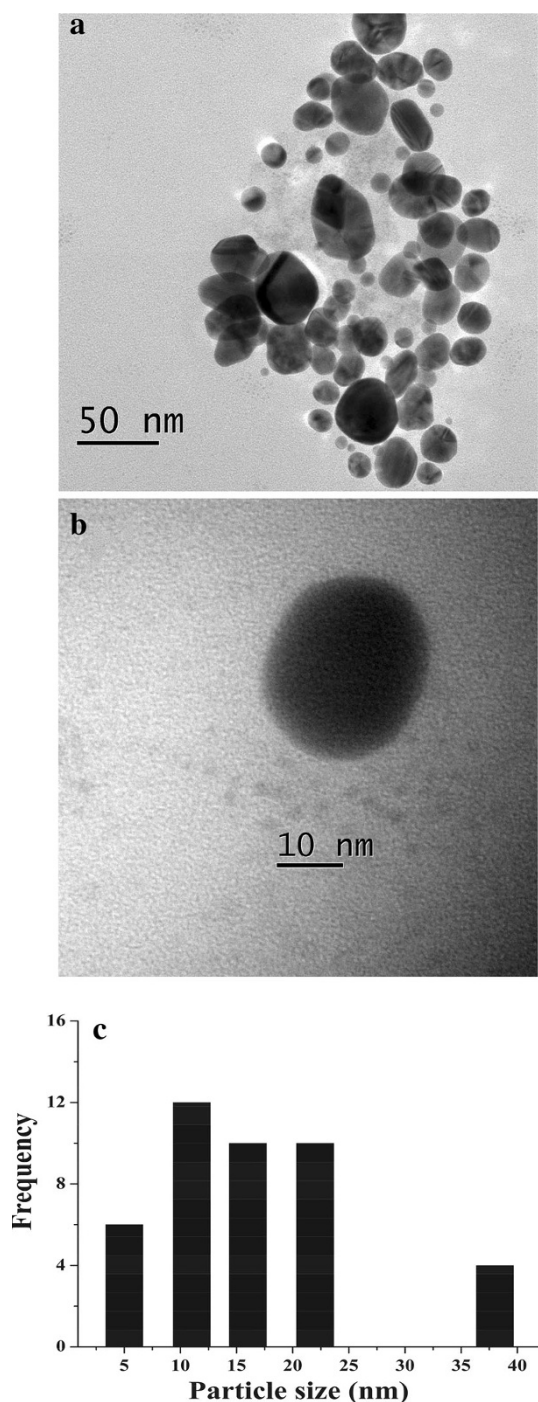


Fig. 4 TEM images of gold nanoparticles at **a** low magnification and **b** high magnification prepared by 0.01 M (Au^{3+}) concentration. **c** Particle size histogram gives the size distribution of gold nanoparticles using TEM

nonspherical nature of the gold nanoparticles. The second absorption band may also arise due to nanoparticle aggregation. When the particles are in close proximity, the

electromagnetic field of one particle influences its plasmon, leading to plasmon absorption at longer wavelength because of the collective plasmon oscillation of the aggregated system. The frequency and intensity of the second band depend on the degree of aggregation and orientation of the individual particle within the aggregate (Munro et al. 1995). The expected agglomeration could be seen in the nanoparticles on increasing the concentration of Au^{3+} ions which may lead to the increase of the grain size. The increase in the particle size due to agglomeration is associated with the red shift of the surface plasmon resonance band (Serrano et al. 2008). An absorption band ~ 330 nm (Fig. 5a–f) is due to presence of the absorption of unreduced gold ions (Serrano et al. 2008), whereas the band at ~ 400 nm may be assigned to the higher order plasmon resonance of the anisotropic gold nanoparticles (Kelly et al. 2003).

BET surface area studies

The BET gas adsorption method is used for the determination of the surface area of the gold nanoparticles. Figure 6 shows the BET plots of the gold nanoparticles prepared in the TritonX-100 based microemulsions at different concentrations of the gold salt. The specific surface areas of the gold nanoparticles were determined using the multiple point BET equation as shown in Table 1. As can be seen from the table, the specific surface area of the gold nanoparticles increases from 5.8 to 107 m^2/g as the concentration of the gold salt decreases from 0.1 to 0.01 M. Thus, the surface area varies with the variation of the particle size obtained using the TEM studies and well corroborated with the size studies. Assuming the particles to have a spherical shape with smooth surface and same size, the surface area can be related to the average equivalent particle size by the equation: $D_{\text{BET}} = 6,000/(\rho \times S_w)$ (in nm), where D_{BET} is the average diameter of a spherical particle, S_w represents the measured surface area of the powder in m^2/g and ρ is the theoretical density of gold ($19.28 \text{ g}/\text{cm}^3$) (Wani et al. 2010; Haiss et al. 2007). The particle size of the gold nanoparticles was then calculated from their corresponding specific surface areas using the above equation (Table 1). As can be seen, the particle size decreases from 53.7 to 2.9 nm as the molar concentration of the gold salt decreases regularly from 0.1 to 0.01 M. The particle size obtained from the BET studies has the same trend as obtained from the TEM studies. However, the difference in size values of BET and TEM could be observed which might be associated to the TEM specimen preparation and degassing process for the measurement of the surface area studies.

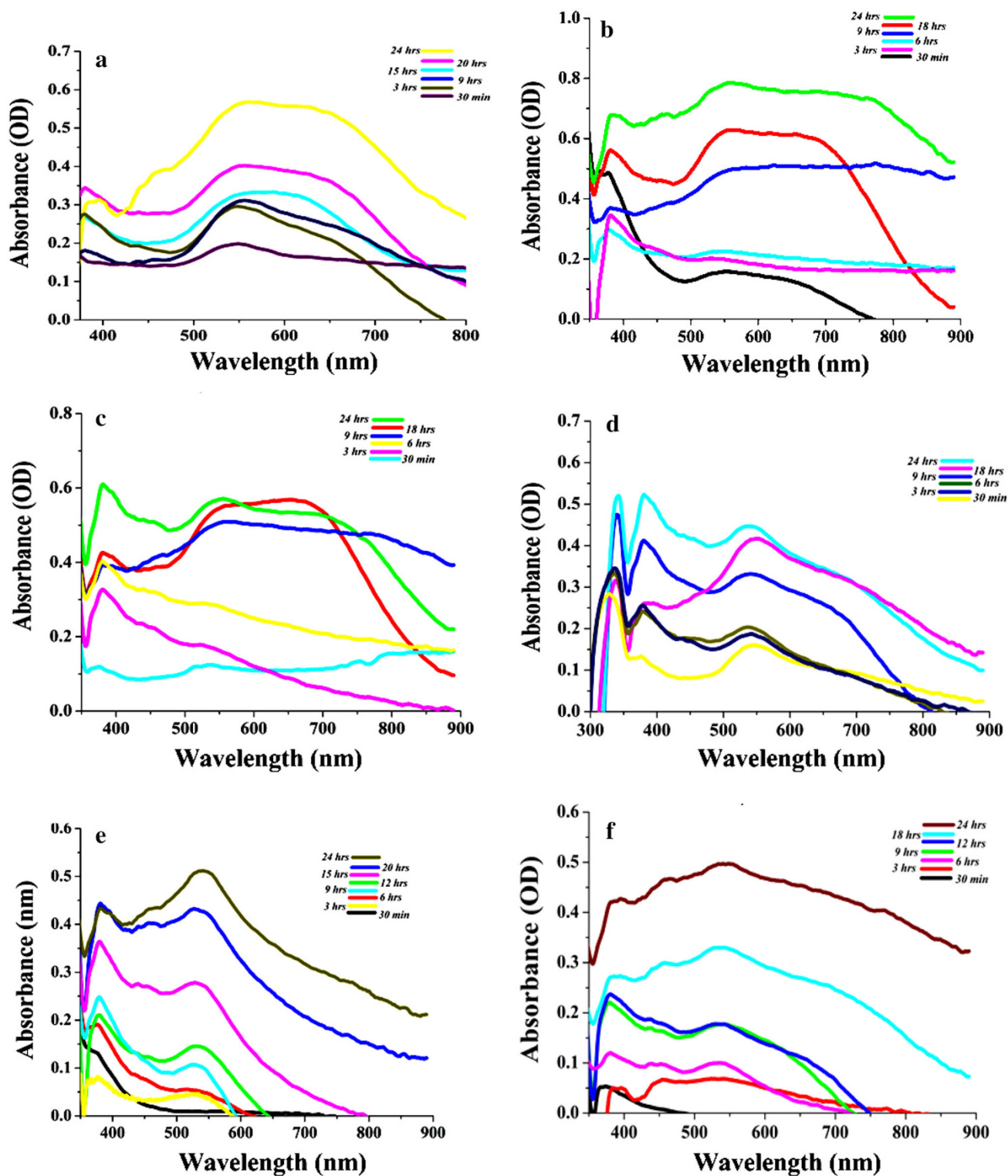


Fig. 5 Time resolved UV–Visible absorption spectra of gold nanoparticles prepared at **a** 0.1 M, **b** 0.05 M, **c** 0.04 M, **d** 0.03 M, **e** 0.02 M and **f** 0.01 M concentrations of Au^{3+}

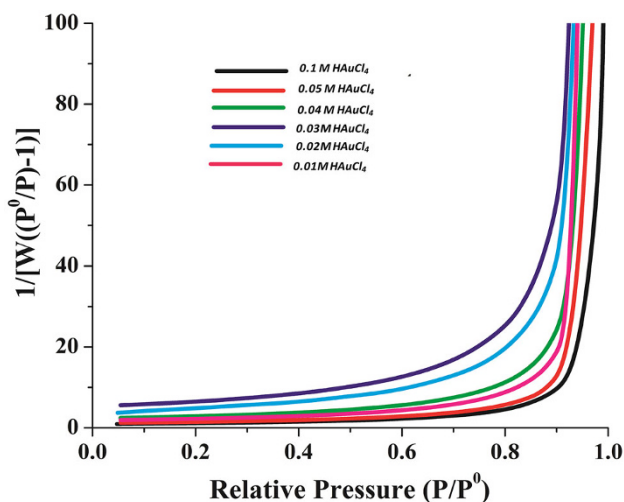


Fig. 6 BET plots of gold nanoparticles prepared at different (0.1, 0.05, 0.04, 0.03, 0.02 and 0.01 M) concentrations of HAuCl₄

Table 1 BET surface area, BET and TEM particle size of gold nanoparticles at different concentrations of Au³⁺ in TritonX-100 based microemulsions

S. no.	Concentration of Au ³⁺ (M)	Specific surface area (m ² /g)	BET size (nm) $D_{BET} = 6,000/(\rho S_w)$	TEM size (nm)
1	0.1	5.8	53.7	60
2	0.05	12.6	24.7	50
3	0.04	16.7	18.6	40
4	0.03	22.4	13.9	35
5	0.02	55	5.7	25
6	0.01	107	2.9	15

Conclusions

Highly crystalline and monophasic gold nanoparticles were successfully prepared in TritonX-100 based inverse microemulsions at different concentrations of Au³⁺ ions. TEM studies show the systematic variation in particle size with change in concentration of gold salt inside the microemulsion. UV–Visible spectroscopy shows the characteristic surface plasmon resonance peak at ~540 nm. The bands appeared at shorter and longer wavelengths of the surface plasmon peak indicate the higher order transitions in gold nanoparticles. The surface area studies show that the surface area increases from 5.8 to 107 m²/g with decrease in the concentration of gold salt from 0.1 to 0.01 M which corroborates well with the particle sizes obtained from the TEM studies.

Acknowledgments TA thanks to Department of Science and Technology (DST) for the financial support (SR/FTP/CS-120/2006).

The authors thank Professor Ashok K. Ganguli for the use of HRTEM facility (funded by DST, Nano Mission) at IIT Delhi.

Open Access This article is distributed under the terms of the Creative Commons Attribution License which permits any use, distribution, and reproduction in any medium, provided the original author(s) and the source are credited.

References

- Ahmad T, Ganguli AK (2004) Synthesis of nanometer-sized particles of barium orthotitanate prepared through a modified reverse micellar route: structural characterization, phase stability and dielectric properties. *J Mater Res* 19:2905–2912
- Ahmad T, Ramanujachary KV, Lofland SE, Ganguli AK (2004) Nanorods of manganese oxalate: a single source precursor to different manganese oxide nanoparticles (MnO, Mn₂O₃, Mn₃O₄). *J Mater Chem* 14:3406–3410
- Ahmad T, Chopra R, Ramanujachary KV, Lofland SE, Ganguli AK (2005) Nanorods of copper and nickel oxalates synthesized by the reverse micellar route. *J Nanosci Nanotechnol* 5:1840–1845
- Ahmad T, Vaidya S, Sarkar N, Ghosh S, Ganguli AK (2006) Zinc oxalate nanorods: a convenient precursor to uniform nanoparticles of ZnO. *Nanotechnology* 17:1236–1240
- Ahmad T, Wani IA, Lone IH, Ganguly A, Manzoor N, Ahmad A, Ahmed J, Al-Shihri AS (2013) Antifungal activity of gold nanoparticles prepared by solvothermal method. *Mater Res Bull* 48:12–20
- Al-Hartomy OA, Ubaidullah M, Khatoon S, Madani JH, Ahmad T (2012) Synthesis, characterization and dielectric properties of nanocrystalline Ba_{1-x}Pb_xZrO₃ (0 ≤ x ≤ 0.75) by polymeric citrate precursor route. *J Mater Res* 27:2479–2488
- Alivisatos AP (1996) Semiconductor clusters, nanocrystals, and quantum dots. *Science* 271:933–937
- Antunez-Garcia J, Mejia-Rosales S, Perez-Tijerina E, Montejano-Carrizales JM, Jose-Yacaman M (2011) Coalescence and collisions of gold nanoparticles. *Materials* 4:368–379
- Arcidiacono S, Bieri NR, Poulikakos D, Grigoropoulos CP (2004) On the coalescence of gold nanoparticles. *Int J Multiph Flow* 30:979–994
- Brust M, Walker M, Bethell D, Schiffrin DJ, Whyman RJ (1994) Synthesis of thiol-derivatized gold nanoparticles in a two phase liquid system. *J Chem Soc Chem Commun* 801–802
- Burda C, Chen X, Narayanan R, El-Sayed MA (2005) Chemistry and properties of nanocrystals of different shapes. *Chem Rev* 105:1025–1106
- Chen J, Wiley B, Li ZY, Campbell D, Saeki F, Cang H, Au L, Lee J, Li XD, Xia YN (2005) Gold nanocages: engineering their structure for biomedical applications. *Adv Mater* 17:2255–2261
- Chithrani DB, Jelveh S, Jalali F, Prooijen MV, Allen C, Bristow RG, Hill RP, Jaffray DA (2010) Gold nanoparticles as radiation sensitizers in cancer therapy. *Radiat Res* 173:719–728
- Colvin VL, Schlamp MC, Alivisatos AP (1994) Light-emitting diodes made from cadmium selenide nanocrystals and a semiconducting polymer. *Nature* 370:354–357
- Daniel MC, Astruc D (2004) Gold nanoparticles: assembly, supramolecular chemistry, quantum-size-related properties and applications toward biology, catalysis, and nanotechnology. *Chem Rev* 104:293–346
- Deng JP, Wu C, Yang GH, Mou CY (2005) Pyrene-assisted synthesis of size-controlled gold nanoparticles in sodium dodecyl sulfate micelles. *Langmuir* 21:8947–8951

- Epifani M, Giannini C, Tapfer L, Vasanelli L (2000) Sol–Gel synthesis and characterization of Ag and Au nanoparticles in SiO_2 , TiO_2 , and ZrO_2 thin films. *J Am Ceram Soc* 83:2385–2393
- Frens G (1973) Controlled nucleation for the regulation of particle size in monodisperse gold solutions. *Nat Phys Sci* 241:20–22
- Ganguli AK, Ahmad T (2007) Nanorods of iron oxalate synthesized using reverse micelles: facile route for Fe_2O_3 and Fe_3O_4 nanoparticles. *J Nanosci Nanotechnol* 7:2029–2035
- Gracias DH, Tien J, Breen TL, Hsu C, Whitesides GM (2000) Formation of electrical networks in three dimensions by self assembly. *Science* 289:1170–1172
- Gul IH, Ahmed W, Maqsood A (2008) Electrical and magnetic characterization of nanocrystalline Ni–Zn ferrite synthesis by co-precipitation route. *J Magn Magn Mater* 320:270–275
- Haba Y, Kojima C, Harada A, Ura T, Horinaka H, Kono K (2007) Preparation of poly (ethylene glycol) modified poly (amido amine) dendrimers encapsulating gold nanoparticles and their heat generating capacity. *Langmuir* 23:5243–5246
- Haiss W, Tharh NTK, Aveyard J, Fernig DG (2007) Determination of size and concentration of gold nanoparticles from UV-Vis spectra. *Anal Chem* 79:4215–4221
- Huang H, Yang X (2004) Synthesis of chitosan-stabilized gold nanoparticles in the absence/presence of tripoly phosphate. *Biomacromolecules* 5:2340–2346
- Huang X, Jain PK, El-Sayed IH, El-Sayed MA (2006) Determination of the minimum temperature required for selective photothermal destruction of cancer cells with the use of immunotargeted gold nanoparticles. *Photochem Photobiol* 82:412–417
- Kamat PV (1998) Nanoparticles and nanostructured films. In: Fendler JH (ed) Wiley, New York, p 207
- Kaushik P, Vaidya S, Ahmad T, Ganguli AK (2007) Optimizing the hydrodynamic radii and polydispersity of reverse-micelles in the Triton X-100–water–cyclohexane system using dynamic light scattering and other studies. *Colloids Surf A Physicochem Eng Aspects* 293:162–166
- Kelly KL, Coronado E, Zhao LL, Schatz GC (2003) The optical properties of metal nanoparticles: the influence of size, shape and dielectric environment. *J Phys Chem B* 107:668–677
- Kuo CH, Chiang TF, Chen LJ, Huang MH (2004) Synthesis of highly faceted pentagonal and hexagonal shaped gold nanoparticles with controlled sizes by sodium dodecyl sulphate. *Langmuir* 20:7820–7824
- Lee MH, Oh SG, Suh KD, Kim DG, Sohn D (2002) Preparation of silver nanoparticles in hexagonal phase formed by nonionic Triton X-100 surfactant. *Colloids Surf A: Physicochem Eng Asp* 210:49–60
- Mansur HS, Grieser F, Marychurch MS, Biggs S, Urquhart RS, Furlong DN (1995) Photoelectrochemical properties of Q-state CdS particles in arachidic acid Langmuir–Blodgett films. *J Chem Soc Faraday Trans* 91:665–672
- Munro CH, Smith WE, Garner M, Clarkson J, White PC (1995) Characterization of the surface of a citrate-reduced colloid optimized for use as a substrate for surface-enhanced resonance Raman scattering. *Langmuir* 11:3712–3720
- Niemeyer CM (2001) Nanoparticles, proteins and nucleic acids: biotechnology meets materials science. *Angewandte Chemie International Edition* 40:4128–4158
- Sastry M, Ahmad A, Khan MI, Kumar R (2003) Biosynthesis of metal nanoparticles using fungi and actinomycete. *Curr Sci* 85:162–170
- Serrano G, Pal U, Herera AM, Salas P, Chavez CA (2008) One step “green” synthesis and stabilization of Au and Ag nanoparticles using ionic polymers. *Chem Mater* 20:5146–5153
- Spirin MG, Brichkin SB, Razumov VF (2005) Synthesis and stabilization of gold nanoparticles in reverse micelles of aerosol OT and Triton X-100. *Colloid J* 67:485–490
- Takahashi H, Niidome Y, Yamada S (2005) Controlled release of plasmid DNA from gold nanorods induced by pulsed near-infrared light. *Chem Commun* 2247–2249
- Tripathy P, Mishra A, Ram S (2007) Immobilizing Au-nanocolloids in Co-branched polymer molecules in presence of gluconic acid in poly (vinyl alcohol) in hot water. *Mater Chem Phys* 106:379–386
- Turkevich J, Stevenson PC, Hillier J (1951) A study of nucleation and growth process in the synthesis of colloidal gold. *Discuss Faraday Soc* 11:55–57
- Valden M, Lai X, Goodman DW (1998) Onset of catalytic activity of gold clusters on titania with the appearance of nonmetallic properties. *Science* 281:1647–1650
- Wagner J, Kohler JM (2005) Continuous synthesis of gold nanoparticles in a microreactor. *Nano Lett* 5:685–691
- Wani IA, Ahmad T (2013) Size and shape dependant antifungal activity of gold nanoparticles: a case study of Candida. *Colloids Surf B Biointerfaces* 101:162–170
- Wani IA, Khattoon S, Ganguly A, Ahmed J, Ganguli AK, Ahmad T (2010) Silver nanoparticles: large scale solvothermal synthesis and optical properties. *Mater Res Bull* 45:1033–1038
- Wani IA, Ganguly A, Ahmed J, Ahmad T (2011) Silver nanoparticles: ultrasonic wave assisted synthesis, optical characterization and surface area studies. *Mater Lett* 65:520–522
- Wani IA, Khattoon S, Ganguly A, Ahmed J, Ahmad T (2013) Structural characterization and antimicrobial properties of silver nanoparticles prepared by inverse microemulsion method. *Colloids Surf B Biointerfaces* 101:243–250
- Yoffe AD (1993) Low dimensional systems: quantum size effects and electronic properties of semiconductor microcrystallites (zero dimensional systems) and some quasi-two-dimensional systems. *Adv Phys* 42:173–262
- Zhang X, Chan KY (2002) Microemulsion synthesis and electrocatalytic properties of platinum-cobalt nanoparticles. *J Mater Chem* 12:1203–1206
- Zhang X, Chan KY (2003) Water-in-oil microemulsion synthesis of platinum-ruthenium nanoparticles, their characterization and electrocatalytic properties. *Chem Mater* 15:451–459